J Sci Comput (2009) 41: 300–320
DOI 10.1007/s10915-009-9299-8

Guidelines for Poisson Solvers on Irregular Domains with Dirichlet Boundary Conditions Using the Ghost Fluid Method

Yen Ting Ng · Han Chen · Chohong Min · Frédéric Gibou

Received: 27 November 2007 / Revised: 7 November 2008 / Accepted: 1 May 2009 / Published online: 8 May 2009

Abstract We consider the variable coefficient Poisson equation with Dirichlet boundary conditions on irregular domains. We present numerical evidence for the accuracy of the solution and its gradients for different treatments at the interface using the Ghost Fluid Method for Poisson problems of Gibou *et al*. (J. Comput. Phys. 176:205–227, 2002; 202:577–601, 2005). This paper is therefore intended as a guide for those interested in using the GFM for Poisson-type problems (and by consequence diffusion-like problems and Stefan-type problems) by providing the pros and cons of the different choices for defining the ghost values and locating the interface. We found that in order to obtain second-order-accurate gradients, both a quadratic (or higher order) extrapolation for defining the ghost values and a quadratic (or higher order) interpolation for finding the interface location are required. In the case where the ghost values are defined by a linear extrapolation, the gradients of the solution converge slowly (at most first order in average) and the convergence rate oscillates, even when the interface location is defined by a quadratic interpolation. The same conclusions hold true for the combination of a quadratic extrapolation for the ghost cells and a linear interpolation. The solution is second-order accurate in all cases. Defining the ghost values with quadratic extrapolations leads to a non-symmetric linear system with a worse conditioning than that of the linear extrapolation case, for which the linear system is symmetric and better conditioned. We conclude that for problems where only the solution matters, the method described by Gibou, F., Fedkiw, R., Cheng, L.-T. and Kang, M. in (J. Comput. Phys. 176:205–227, 2002) is advantageous since the linear system that needs to be inverted is symmetric. In problems where the solution gradient is needed, such as in Stefan-type problems,

Y.T. Ng · H. Chen
Computer Science Department, University of California, Santa Barbara, CA 93106, USA

C. Min (✉)
Mathematics Department and Research Institute for Basic Sciences, KyungHee University, Seoul, Korea 130-701
e-mail: chohong@khu.ac.kr

F. Gibou
Mechanical Engineering Department & Computer Science Department, University of California, Santa Barbara, CA 93106, USA

higher order extrapolation schemes as described by Gibou, F. and Fedkiw, R. in (J. Comput. Phys. 202:577–601, 2005) are desirable.

Keywords Level set · Ghost fluid method · Poisson equation · Irregular domains

1 Introduction

The Ghost Fluid Method (GFM), introduced by Fedkiw *et al.* in the context of compressible gas dynamics [4] is an important numerical technique developed to implicitly impose sharp boundary conditions on an irregular interface. In Liu *et al.* [13] the Ghost Fluid Method was used to guide the development of a first-order-accurate symmetric discretization of the variable coefficient Poisson equation in the presence of an irregular domain, where the variable coefficients, the solution and the derivatives of the solution may have jumps across the interface. In Kang *et al.* [11] and Nguyen *et al.* [15], this method was applied to two-phase incompressible flows and to incompressible flame front discontinuities, respectively. A second-order accurate symmetric discretization was developed in Gibou *et al.* [8] for the variable coefficient Poisson equation on irregular domains with Dirichlet boundary conditions instead of jump conditions. This discretization was then extended to fourth-order accuracy in Gibou *et al.* [6]. The discretizations proposed in [13] and in [8] both yield symmetric linear systems that can readily be inverted with a number of fast methods, such as a Preconditioned Conjugate Gradient (PCG) method (see e.g. Golub and Van Loan [9, 16]). This is an advantage over the original level set method for solving the Stefan problem by Chen *et al.* [1] who proposed a non-symmetric scheme. Likewise, a second-order accurate method for the jump condition case was developed in Li *et al.* [12] but with a non-symmetric discretization matrix.

The symmetric discretization presented in [8] has been successfully applied to the simulation of free surface flows in Enright *et al.* [3], multiphase flows with phase-change in Gibou *et al.* [5] and the Stefan Problem in Gibou *et al.* [7]. In this paper, we further analyze the order of accuracy and error distribution of the gradients produced by the method of Gibou *et al.* [6, 8]. The goal of this paper is therefore to provide a 'how-to' on the choices one can make when considering the Poisson equation on irregular domains with Dirichlet boundary conditions. Since the same techniques can be applied to diffusion-like as well as Stefan-type problems, this paper can serve as a guide for those problems as well.

In a nutshell, the disadvantage of using a quadratic extrapolation for the ghost value is that the associated linear system is no longer symmetric, as it is the case for [1, 6], and that the condition number of the matrix is significantly larger than that of symmetric discretizations. On the other hand, defining ghost values with quadratic extrapolations (or higher) leads to more accurate computations of the gradients, which in turn impacts the accuracy of moving boundary problems with velocity defined from the solution gradients. Our results are in agreement with the analytical expression for the error in one spatial dimension presented in Jomaa *et al.* [10] for both the linear and quadratic boundary treatments and the observation in McCorquodale *et al.* [14] that a quadratic treatment at the interface leads to second-order accuracy for the solution gradients.

2 Equations and Numerical Methods

2.1 Poisson Equation

Consider a Cartesian computational domain, $\Omega \in R^n$, with exterior boundary, $\partial\Omega$ and a lower dimensional interface Γ that divides the computational domain into disjoint pieces, Ω^- and Ω^+. The variable coefficient Poisson equation is given by

$$\nabla \cdot (\beta(\vec{x})\nabla u(\vec{x})) = f(\vec{x}), \quad \vec{x} \in \Omega, \tag{1}$$

where $\vec{x} = (x, y, z)$ is the vector of spatial coordinates and $\nabla = (\frac{\partial}{\partial x}, \frac{\partial}{\partial y}, \frac{\partial}{\partial z})$ is the gradient operator. The variable coefficient $\beta(\vec{x})$ is assumed to be continuous on each disjoint subdomain, Ω^- and Ω^+, but may be discontinuous across the interface Γ. $\beta(\vec{x})$ is further assumed to be positive and bounded below by some $\epsilon > 0$. On $\partial\Omega$, either Dirichlet boundary conditions of $u(\vec{x}) = g(\vec{x})$ or Neumann boundary conditions of $u_n(\vec{x}) = h(\vec{x})$ are specified. Here $u_n = \nabla u \cdot \vec{n}$ is the normal derivative of u and $\vec{n}$ is the outward normal to the interface. A Dirichlet boundary condition of $u = u_I$ is imposed on Γ.

In order to separate the different subdomains, we introduce a level set function ϕ defined as the signed distance function:

$$\begin{cases} \phi = -d & \text{for } \vec{x} \in \Omega^-, \\ \phi = +d & \text{for } \vec{x} \in \Omega^+, \\ \phi = 0 & \text{for } \vec{x} \in \Gamma, \end{cases}$$

where d is the distance to the interface. The level set is used to identify the location of the interface as well as the interior and exterior regions.

2.2 Discretization of the Poisson Equation on Irregular Domains

In this section, we recall the discretization of the Poisson equation on irregular domains, as described in Gibou *et al.* [6, 8]. The discretization of the Poisson equation, including the special treatments needed at the interface, is performed in a dimension by dimension fashion. Therefore, without loss of generality, we only describe the discretization in one spatial dimension for the $(\beta u_x)_x$ term. In multiple spatial dimensions, the $(\beta u_y)_y$ and $(\beta u_z)_z$ terms are each independently discretized in the same manner as $(\beta u_x)_x$.

Consider the variable coefficient Poisson equation in one spatial dimension

$$(\beta u_x)_x = f, \tag{2}$$

with Dirichlet boundary conditions of $u = u_I$ on the interface where $\phi = 0$. The computational domain is discretized into cells of size Δx with the grid nodes x_i located at the cell centers. The cell edges are referred to as fluxes so that the two fluxes bounding the grid node x_i are located at $x_{i\pm\frac{1}{2}}$. The solution of the Poisson equation is computed at the grid nodes and is written as $u_i = u(x_i)$. We consider the standard second-order discretization for (2) given by

$$\frac{\beta_{i+\frac{1}{2}}(\frac{u_{i+1}-u_i}{\Delta x}) - \beta_{i-\frac{1}{2}}(\frac{u_i-u_{i-1}}{\Delta x})}{\Delta x} = f_i, \tag{3}$$

where $(\beta u)_x$ is discretized at the flux locations.

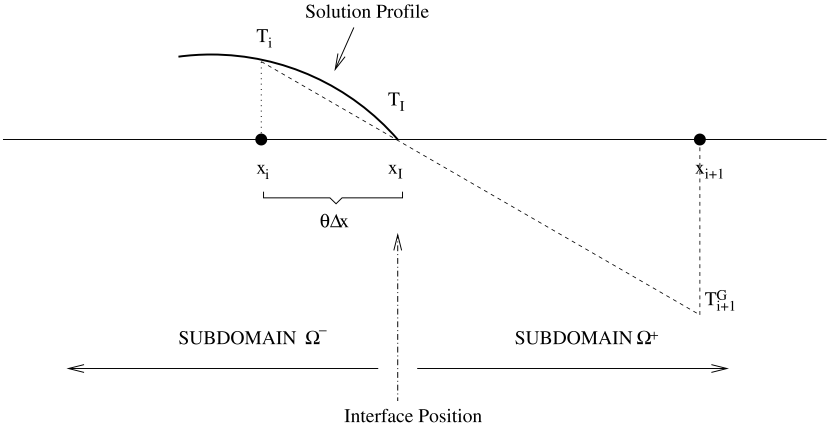

Fig. 1 Definition of the ghost cells with linear extrapolation. First, we construct a linear interpolant $\tilde{u}(x) = ax + b$ of u such that $\tilde{u}(0) = u_i$ and $\tilde{u}(\theta\Delta x) = u_I$. Then we define $u^G_{i+1} = \tilde{u}(\Delta x)$

In order to avoid differentiating the fluxes across the interface where the solution presents a kink, a ghost value is used: Referring to Fig. 1, let x_I be an interface point between grid points x_i and x_{i+1} with a Dirichlet boundary condition of $u = u_I$ applied at x_I. We define a ghost value u^G_{i+1} at x_{i+1} across the interface, and rewrite (3) as

$$\frac{\beta_{i+\frac{1}{2}}(\frac{u^G_{i+1}-u_i}{\Delta x}) - \beta_{i-\frac{1}{2}}(\frac{u_i-u_{i-1}}{\Delta x})}{\Delta x} = f_i. \tag{4}$$

The ghost value u^G_{i+1} is defined by first constructing an interpolant $\tilde{u}(x)$ of $u(x)$ on the left of the interface, such that $\tilde{u}(0) = u_i$, and then defining $u^G_{i+1} = \tilde{u}(\Delta x)$. Figure 1 illustrates the definition of the ghost cells in the case of the linear extrapolation. In this work, we consider linear and quadratic extrapolations defined by:

Linear extrapolation: Take $\tilde{u}(x) = ax + b$ with:

- $\tilde{u}(0) = u_i$,
- $\tilde{u}(\theta\Delta x) = u_I$.

Quadratic extrapolation: Take $\tilde{u}(x) = ax^2 + bx + c$ with:

- $\tilde{u}(-\Delta x) = u_{i-1}$,
- $\tilde{u}(0) = u_i$,
- $\tilde{u}(\theta\Delta x) = u_I$,

where $\theta \in [0, 1]$ refers to the cell fraction occupied by the subdomain Ω^-.

2.3 Location of the Interface

Referring to Fig. 1, we compute the location of the interface between x_i and x_{i+1} by finding the zero crossing of the quadratic interpolant $\phi = \phi(x_i) + \phi_x(x_i)x + \frac{1}{2}\phi_{xx}(x_i)x^2$. We note that the quadratic interpolant in ϕ is convex with a positive second order derivative.

The location of the interface along the x-direction is calculated as:

$$\theta\Delta x = \begin{cases} \frac{-\phi_x(x_i)+\sqrt{\phi_x^2(x_i)-2\phi_{xx}(x_i)\phi(x_i)}}{\phi_{xx}(x_i)} & \text{if } \phi_{xx}(x_i) > \epsilon, \\ -\frac{\phi(x_i)}{\phi_x(x_i)} & \text{if } |\phi_{xx}(x_i)| \le \epsilon, \end{cases} \tag{5}$$

where ϵ is a small positive number to avoid division by zero. $\phi_x(x_i)$ and $\phi_{xx}(x_i)$ are approximated at x_i using second-order accurate central difference schemes.

2.4 Computation of the Gradients

The solution gradients are computed at each node of the grid: Once we know the location of the interface as described in Sect. 2.3, the Dirichlet boundary value u_I is either given analytically or calculated by quadratic interpolation using neighboring nodal values. Then central-type difference schemes using the value at the interface are used to approximate the component of $\nabla u = (u_x, u_y, u_z)^T$. For example, we define u_x as

$$u_x = \frac{u_I - u_i}{\theta\Delta x}\frac{1}{1+\theta} + \frac{u_i - u_{i-1}}{\Delta x}\frac{\theta}{1+\theta}.$$

We note that in the case where x_{i-1} is outside the domain, we recourse to a first-order formula. Likewise, if θ is too small, we set $u_i = u_I$ to remove the large errors that could occur from dividing by small numbers. In practice we set the threshold to be $\theta = \Delta x$.

Remarks

- The GFM for the Poisson equation produces second-order accurate solutions even in the case where the interface cuts two adjacent segments (in a least square fit sense).
- The accuracy of the gradient is also second order in the case where the interface and the extrapolation are second-order accurate. Same conclusions are reached in the approach of Chern and Shu [2].

3 Examples

In each example, we consider a domain $\Omega = [-2, 2]^2$ and $\Delta u = f$ on Ω. The level set function ϕ decomposes the domain into separate regions, with $\phi = 0$ defining the interface Γ. The interior region Ω^- is defined by $\phi \le 0$ while the exterior region Ω^+ is defined by $\phi > 0$. We impose Dirichlet boundary conditions on both the exterior boundary $\partial\Omega$ and the interface Γ. We use the BiCGSTAB algorithm with an incomplete LU preconditioner to solve the linear systems, although one would choose more efficient solvers in practice (for example PCG in the case of symmetric linear systems, GMRES or multigrid methods in the case of non symmetric linear systems). In the examples below, we show the results with different combinations for the definition of the ghost cells and the interpolation to locate the interface. In addition, we present those results in the case where the interface may or may not be smooth, as well as in the case of perturbation of the interface on the grid.

3.1 Numerical Results for a Disk-Shaped Irregular Domain

In this example, the interface Γ is a circle. We use an exact solution of $u(x,y)=e^{\phi}$. We define ϕ as $\phi(x,y)=(x-px)^2+(y-py)^2-1$, where px and py are randomly chosen perturbations. We consider the case with $px=0$ and $py=0$ where the circle is centered at the origin, and also the case with $px=0.691$ and $py=0.357$ so that the center of the circle does not fall exactly on a grid point. Figure 2 depicts the grids used and the exact solution. The L^∞ errors in the solution and gradient are presented in Tables 1 through 8.

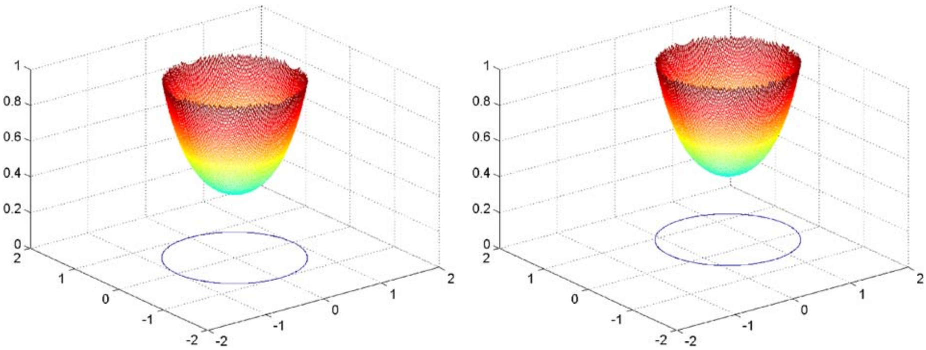

Fig. 2 Example 3.1 grids and exact solution at 256^2 resolution. The figure *on the left* depicts the case where the circle is centered, while the figure *on the right* depicts the case where *the center of the circle* is perturbed

Table 1 Example 3.1 centered circle. Maximum error for the solution and its gradients in the case where the ghost value is defined by a *linear* extrapolation and the interface location is found with a *linear* interpolant

Effective resolution	$\|u-u_h\|_\infty$	Order	$\|\nabla u-\nabla u_h\|_\infty$	Order
32^2	3.34×10^{-3}	–	9.91×10^{-2}	–
64^2	1.24×10^{-3}	1.43	6.63×10^{-2}	0.58
128^2	3.66×10^{-4}	1.76	5.20×10^{-2}	0.35
256^2	1.03×10^{-4}	1.83	2.90×10^{-2}	0.84
512^2	2.73×10^{-5}	1.92	1.27×10^{-2}	1.19
1024^2	7.11×10^{-6}	1.94	8.10×10^{-3}	0.65

Table 2 Example 3.1 centered circle. Maximum error for the solution and its gradients in the case where the ghost value is defined by a *linear* extrapolation and the interface location is found with a *quadratic* interpolant

Effective resolution	$\|u-u_h\|_\infty$	Order	$\|\nabla u-\nabla u_h\|_\infty$	Order
32^2	6.17×10^{-3}	–	1.99×10^{-1}	–
64^2	2.05×10^{-3}	1.59	1.17×10^{-1}	0.76
128^2	5.68×10^{-4}	1.85	9.92×10^{-2}	0.24
256^2	1.57×10^{-4}	1.85	5.28×10^{-2}	0.91
512^2	4.13×10^{-5}	1.93	2.37×10^{-2}	1.16
1024^2	1.07×10^{-5}	1.95	1.53×10^{-2}	0.63

Table 3 Example 3.1 centered circle. Maximum error for the solution and its gradients in the case where the ghost value is defined by a *quadratic* extrapolation and the interface location is found with a *linear* interpolant

Effective resolution	$\|u - u_h\|_\infty$	Order	$\|\nabla u - \nabla u_h\|_\infty$	Order
32^2	7.59×10^{-3}	–	7.69×10^{-2}	–
64^2	2.12×10^{-3}	1.84	4.51×10^{-2}	0.77
128^2	5.30×10^{-4}	2.00	4.29×10^{-2}	0.07
256^2	1.37×10^{-4}	1.95	2.37×10^{-2}	0.86
512^2	3.42×10^{-5}	2.00	1.09×10^{-2}	1.11
1024^2	8.66×10^{-6}	1.98	6.95×10^{-3}	0.65

Table 4 Example 3.1 centered circle. Maximum error for the solution and its gradients in the case where the ghost value is defined by a *quadratic* extrapolation and the interface location is found with a *quadratic* interpolant

Effective resolution	$\|u - u_h\|_\infty$	Order	$\|\nabla u - \nabla u_h\|_\infty$	Order
32^2	5.43×10^{-3}	–	2.08×10^{-2}	–
64^2	1.44×10^{-3}	1.91	6.46×10^{-3}	1.69
128^2	3.81×10^{-4}	1.92	2.10×10^{-3}	1.62
256^2	9.72×10^{-5}	1.97	5.59×10^{-4}	1.91
512^2	2.46×10^{-5}	1.98	1.30×10^{-4}	2.11
1024^2	6.19×10^{-6}	1.99	3.76×10^{-5}	1.78

Table 5 Example 3.1 perturbed circle. Maximum error for the solution and its gradients in the case where the ghost value is defined by a *linear* extrapolation and the interface location is found with a *linear* interpolant

Effective resolution	$\|u - u_h\|_\infty$	Order	$\|\nabla u - \nabla u_h\|_\infty$	Order
32^2	5.57×10^{-3}	–	2.46×10^{-1}	–
64^2	1.44×10^{-3}	1.95	1.27×10^{-1}	0.95
128^2	4.34×10^{-4}	1.73	6.39×10^{-2}	0.99
256^2	1.09×10^{-4}	2.00	3.21×10^{-2}	0.99
512^2	2.93×10^{-5}	1.89	1.67×10^{-2}	0.94
1024^2	7.41×10^{-6}	1.99	8.37×10^{-3}	1.00

Table 6 Example 3.1 perturbed circle. Maximum error for the solution and its gradients in the case where the ghost value is defined by a *linear* extrapolation and the interface location is found with a *quadratic* interpolant

Effective resolution	$\|u - u_h\|_\infty$	Order	$\|\nabla u - \nabla u_h\|_\infty$	Order
32^2	9.15×10^{-3}	–	4.98×10^{-1}	–
64^2	2.30×10^{-3}	1.99	2.53×10^{-1}	0.98
128^2	6.63×10^{-4}	1.80	1.23×10^{-1}	1.04
256^2	1.66×10^{-4}	2.00	6.08×10^{-2}	1.02
512^2	4.42×10^{-5}	1.90	3.24×10^{-2}	0.91
1024^2	1.11×10^{-5}	1.99	1.62×10^{-2}	1.00

Table 7 Example 3.1 perturbed circle. Maximum error for the solution and its gradients in the case where the ghost value is defined by a *quadratic* extrapolation and the interface location is found with a *linear* interpolant

Effective resolution	$\|u-u_h\|_\infty$	Order	$\|\nabla u-\nabla u_h\|_\infty$	Order
32^2	7.86×10^{-3}	–	1.75×10^{-1}	–
64^2	2.07×10^{-3}	1.92	1.04×10^{-1}	0.75
128^2	5.48×10^{-4}	1.92	5.30×10^{-2}	0.97
256^2	1.38×10^{-4}	1.98	2.69×10^{-2}	0.98
512^2	3.50×10^{-5}	1.99	1.53×10^{-2}	0.81
1024^2	8.79×10^{-6}	1.99	7.70×10^{-3}	0.99

Table 8 Example 3.1 perturbed circle. Maximum error for the solution and its gradients in the case where the ghost value is defined by a *quadratic* extrapolation and the interface location is found with a *quadratic* interpolant

Effective resolution	$\|u-u_h\|_\infty$	Order	$\|\nabla u-\nabla u_h\|_\infty$	Order
32^2	5.19×10^{-3}	–	3.46×10^{-2}	–
64^2	1.45×10^{-3}	1.84	8.92×10^{-3}	1.96
128^2	3.78×10^{-4}	1.94	2.36×10^{-3}	1.92
256^2	9.71×10^{-5}	1.96	6.01×10^{-4}	1.98
512^2	2.46×10^{-5}	1.98	1.50×10^{-4}	2.00
1024^2	6.18×10^{-6}	1.99	3.85×10^{-5}	1.96

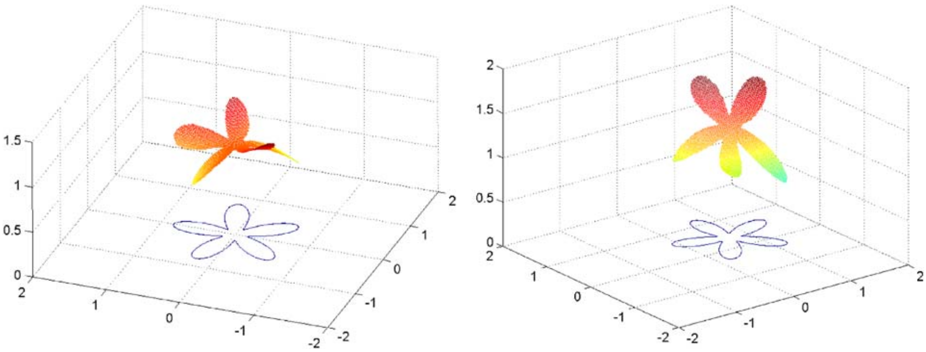

Fig. 3 Example 3.2 grids and exact solution at 256^2 resolution. The figure *on the left* depicts the case where the star is centered, while the figure *on the right* depicts the case where *the center of the star* is perturbed

3.2 Numerical Results for a Star-Shaped Irregular Domain

In this example, the interface Γ is a star, hence considering the case where the irregular domain has a more complex shape. We use an exact solution of $u(x,y)=\sin(x)\sin(y)+1$. We define ϕ as $\phi(x,y)=\sqrt{(x-px)^2+(y-py)^2}-0.5-\frac{(y-py)^5+5(x-px)^4(y-py)-10(x-px)^2(y-py)^3}{3((x-px)^2+(y-py)^2)^2}$ for $\sqrt{(x-px)^2+(y-py)^2}\geq 10^{-4}$ and $\phi(x,y)=-1$ otherwise, where px and py are randomly chosen perturbations. We consider the case with $px=0$ and $py=0$ where the star is centered at the origin, and also the case with $px=0.691$ and $py=0.357$ so that the center of the star does not fall exactly on a grid point. Figure 3 depicts the grids used and the exact solution. The L^∞ errors in the solution and gradient are presented in Tables 9 through 16.

Table 9 Example 3.2 centered star. Maximum error for the solution and its gradients in the case where the ghost value is defined by a *linear* extrapolation and the interface location is found with a *linear* interpolant

Effective resolution	$\|u-u_h\|_\infty$	Order	$\|\nabla u-\nabla u_h\|_\infty$	Order
32^2	3.64×10^{-4}	–	1.35×10^{-2}	–
64^2	1.19×10^{-4}	1.61	1.40×10^{-2}	−0.05
128^2	2.54×10^{-5}	2.23	7.54×10^{-3}	0.89
256^2	8.08×10^{-6}	1.65	3.18×10^{-3}	1.25
512^2	2.01×10^{-6}	2.01	1.64×10^{-3}	0.95
1024^2	4.91×10^{-7}	2.03	9.87×10^{-4}	0.73

Table 10 Example 3.2 centered star. Maximum error for the solution and its gradients in the case where the ghost value is defined by a *linear* extrapolation and the interface location is found with a *quadratic* interpolant

Effective resolution	$\|u-u_h\|_\infty$	Order	$\|\nabla u-\nabla u_h\|_\infty$	Order
32^2	4.12×10^{-4}	–	1.59×10^{-2}	–
64^2	1.20×10^{-4}	1.78	1.56×10^{-2}	0.03
128^2	2.67×10^{-5}	2.17	4.78×10^{-3}	1.71
256^2	8.06×10^{-6}	1.73	3.35×10^{-3}	0.51
512^2	2.01×10^{-6}	2.00	1.67×10^{-3}	1.00
1024^2	4.91×10^{-7}	2.03	9.94×10^{-4}	0.75

Table 11 Example 3.2 centered star. Maximum error for the solution and its gradients in the case where the ghost value is defined by a *quadratic* extrapolation and the interface location is found with a *linear* interpolant

Effective resolution	$\|u-u_h\|_\infty$	Order	$\|\nabla u-\nabla u_h\|_\infty$	Order
32^2	3.41×10^{-5}	–	1.40×10^{-3}	–
64^2	5.86×10^{-6}	2.54	4.06×10^{-4}	1.79
128^2	9.44×10^{-7}	2.63	5.34×10^{-4}	−0.40
256^2	1.21×10^{-7}	2.97	4.01×10^{-5}	3.74
512^2	1.73×10^{-8}	2.80	1.05×10^{-5}	1.93
1024^2	8.51×10^{-9}	1.02	2.17×10^{-5}	−1.05

Table 12 Example 3.2 centered star. Maximum error for the solution and its gradients in the case where the ghost value is defined by a *quadratic* extrapolation and the interface location is found with a *quadratic* interpolant

Effective resolution	$\|u-u_h\|_\infty$	Order	$\|\nabla u-\nabla u_h\|_\infty$	Order
32^2	3.30×10^{-5}	–	1.46×10^{-3}	–
64^2	6.02×10^{-6}	2.46	4.25×10^{-4}	1.78
128^2	9.55×10^{-7}	2.66	1.13×10^{-4}	1.92
256^2	1.22×10^{-7}	2.97	3.36×10^{-5}	1.74
512^2	1.81×10^{-8}	2.75	8.02×10^{-6}	2.07
1024^2	6.18×10^{-9}	1.55	2.21×10^{-6}	1.86

Table 13 Example 3.2 perturbed star. Maximum error for the solution and its gradients in the case where the ghost value is defined by a *linear* extrapolation and the interface location is found with a *linear* interpolant

Effective resolution	$\|u-u_h\|_\infty$	Order	$\|\nabla u-\nabla u_h\|_\infty$	Order
32^2	9.73×10^{-4}	–	2.45×10^{-2}	–
64^2	2.53×10^{-4}	1.94	3.95×10^{-2}	−0.69
128^2	6.39×10^{-5}	1.98	2.82×10^{-2}	0.49
256^2	1.74×10^{-5}	1.87	3.01×10^{-2}	−0.10
512^2	4.46×10^{-6}	1.97	7.66×10^{-3}	1.98
1024^2	1.11×10^{-6}	2.00	1.30×10^{-2}	−0.77

Table 14 Example 3.2 perturbed star. Maximum error for the solution and its gradients in the case where the ghost value is defined by a *linear* extrapolation and the interface location is found with a *quadratic* interpolant

Effective resolution	$\|u-u_h\|_\infty$	Order	$\|\nabla u-\nabla u_h\|_\infty$	Order
32^2	1.03×10^{-3}	–	2.81×10^{-2}	–
64^2	2.57×10^{-4}	2.01	3.30×10^{-2}	−0.23
128^2	6.46×10^{-5}	1.99	1.67×10^{-2}	0.98
256^2	1.74×10^{-5}	1.89	7.63×10^{-3}	1.13
512^2	4.47×10^{-6}	1.96	4.46×10^{-3}	0.78
1024^2	1.11×10^{-6}	2.01	2.18×10^{-3}	1.03

Table 15 Example 3.2 perturbed star. Maximum error for the solution and its gradients in the case where the ghost value is defined by a *quadratic* extrapolation and the interface location is found with a *linear* interpolant

Effective resolution	$\|u-u_h\|_\infty$	Order	$\|\nabla u-\nabla u_h\|_\infty$	Order
32^2	6.35×10^{-5}	–	2.08×10^{-3}	–
64^2	8.15×10^{-6}	2.96	2.33×10^{-3}	−0.16
128^2	1.29×10^{-6}	2.66	1.13×10^{-3}	1.05
256^2	1.93×10^{-7}	2.74	1.66×10^{-4}	2.76
512^2	5.47×10^{-8}	1.82	1.16×10^{-3}	−2.81
1024^2	2.14×10^{-8}	1.35	1.96×10^{-4}	2.56

Table 16 Example 3.2 perturbed star. Maximum error for the solution and its gradients in the case where the ghost value is defined by a *quadratic* extrapolation and the interface location is found with a *quadratic* interpolant

Effective resolution	$\|u-u_h\|_\infty$	Order	$\|\nabla u-\nabla u_h\|_\infty$	Order
32^2	6.45×10^{-5}	–	2.09×10^{-3}	–
64^2	7.84×10^{-6}	3.04	5.91×10^{-4}	1.82
128^2	1.29×10^{-6}	2.60	1.60×10^{-4}	1.89
256^2	2.02×10^{-7}	2.68	3.92×10^{-5}	2.02
512^2	5.21×10^{-8}	1.96	1.06×10^{-5}	1.89
1024^2	1.82×10^{-8}	1.52	2.70×10^{-6}	1.97

3.3 Numerical Results for a Tilted Square Irregular Domain

In this example, the interface Γ is a tilted square, hence considering the case where the interface has a kink. We use an exact solution of $u(x,y)=e^{-x^2-y^2}$. We define ϕ as $\phi(x,y)=\max[\max(|(\hat{x}-px)-(\hat{y}-py)|-1, |(\hat{y}-py)-(\hat{x}-px)|-1), |(\hat{x}-px)+(\hat{y}-py)|-1]$, where $\hat{x}(x,y)=x\cos(\pi\theta)-y\sin(\pi\theta)$ and $\hat{y}(x,y)=x\sin(\pi\theta)+y\cos(\pi\theta)$. θ, px, and py are randomly chosen perturbations. We consider the case with $\theta=0.313$, $px=0$ and $py=0$ where the tilted square is centered at the origin, and also the case with $\theta=0.313$, $px=0.691$ and $py=0.357$ so that the center of the tilted square does not fall exactly on a grid point. θ is chosen such that the tilted square is not symmetric in the x and y directions. Figure 4 depicts the grids used and the exact solution. The L^∞ errors in the solution and gradient are presented in Tables 17 through 24.

3.4 Numerical Results for a Sphere-Shaped Irregular Domain in Three Dimensions

In this example, the interface Γ is defined by a sphere in three dimensions. We use an exact solution of $u(x,y,z)=e^{\phi}$. We define ϕ as $\phi(x,y,z)=(x-px)^2+(y-py)^2+(z-pz)^2-1$, where px, py and pz are randomly chosen perturbations. We consider the case where the sphere is centered at the $(0,0,0)$, and also the case where the sphere is centered at $(0.249, 0.187, 0.356)$ so that the center of the sphere does not fall exactly on a grid point.

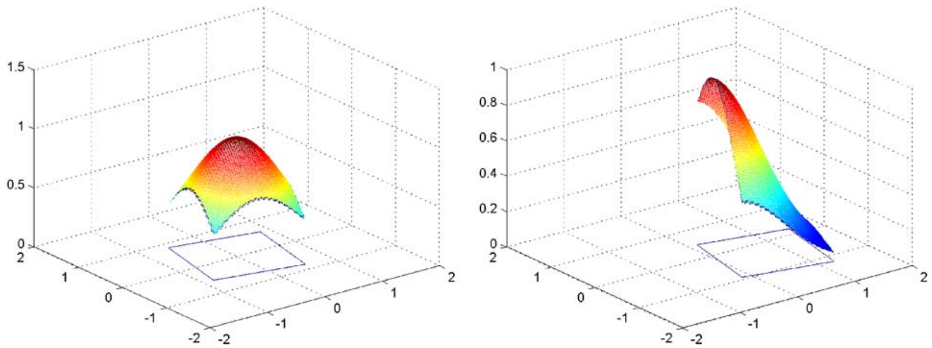

Fig. 4 Example 3.3 grids and exact solution at 256^2 resolution. The figure *on the left* depicts the case where the tilted square is centered, while the figure *on the right* depicts the case where *the center of the tilted square* is perturbed

Table 17 Example 3.3 centered tilted square. Maximum error for the solution and its gradients in the case where the ghost value is defined by a *linear* extrapolation and the interface location is found with a *linear* interpolant

Effective resolution	$\|u-u_h\|_\infty$	Order	$\|\nabla u-\nabla u_h\|_\infty$	Order
32^2	3.22×10^{-3}	–	1.56×10^{-2}	–
64^2	7.75×10^{-4}	2.06	5.75×10^{-3}	1.44
128^2	1.91×10^{-4}	2.02	2.89×10^{-3}	1.00
256^2	4.71×10^{-5}	2.02	3.30×10^{-4}	3.13
512^2	1.17×10^{-5}	2.01	2.74×10^{-4}	0.27
1024^2	2.93×10^{-6}	2.00	2.34×10^{-2}	−6.42

Table 18 Example 3.3 centered tilted square. Maximum error for the solution and its gradients in the case where the ghost value is defined by a *linear* extrapolation and the interface location is found with a *quadratic* interpolant

Effective resolution	$\|u - u_h\|_\infty$	Order	$\|\nabla u - \nabla u_h\|_\infty$	Order
32^2	3.07×10^{-3}	–	1.20×10^{-2}	–
64^2	7.74×10^{-4}	1.99	8.53×10^{-3}	0.50
128^2	1.94×10^{-4}	2.00	8.78×10^{-3}	−0.04
256^2	4.82×10^{-5}	2.01	2.18×10^{-3}	2.01
512^2	1.21×10^{-5}	1.99	1.91×10^{-3}	0.19
1024^2	2.99×10^{-6}	2.02	2.03×10^{-3}	−0.08

Table 19 Example 3.3 centered tilted square. Maximum error for the solution and its gradients in the case where the ghost value is defined by a *quadratic* extrapolation and the interface location is found with a *linear* interpolant

Effective resolution	$\|u - u_h\|_\infty$	Order	$\|\nabla u - \nabla u_h\|_\infty$	Order
32^2	3.15×10^{-3}	–	1.45×10^{-2}	–
64^2	7.75×10^{-4}	2.03	5.75×10^{-3}	1.34
128^2	1.91×10^{-4}	2.02	2.89×10^{-3}	0.99
256^2	4.71×10^{-5}	2.02	3.30×10^{-4}	3.13
512^2	1.17×10^{-5}	2.01	1.35×10^{-4}	1.29
1024^2	2.93×10^{-6}	2.00	2.34×10^{-2}	−7.43

Table 20 Example 3.3 centered tilted square. Maximum error for the solution and its gradients in the case where the ghost value is defined by a *quadratic* extrapolation and the interface location is found with a *quadratic* interpolant

Effective resolution	$\|u - u_h\|_\infty$	Order	$\|\nabla u - \nabla u_h\|_\infty$	Order
32^2	2.74×10^{-3}	–	7.65×10^{-3}	–
64^2	7.15×10^{-4}	1.94	2.14×10^{-3}	1.84
128^2	1.83×10^{-4}	1.97	5.97×10^{-4}	1.84
256^2	4.62×10^{-5}	1.98	1.35×10^{-4}	2.15
512^2	1.16×10^{-5}	1.99	3.79×10^{-5}	1.83
1024^2	2.91×10^{-6}	2.00	8.50×10^{-6}	2.16

Table 21 Example 3.3 perturbed tilted square. Maximum error for the solution and its gradients in the case where the ghost value is defined by a *linear* extrapolation and the interface location is found with a *linear* interpolant

Effective resolution	$\|u - u_h\|_\infty$	Order	$\|\nabla u - \nabla u_h\|_\infty$	Order
32^2	1.51×10^{-3}	–	7.77×10^{-2}	–
64^2	4.43×10^{-4}	1.77	3.40×10^{0}	−5.45
128^2	7.26×10^{-5}	2.61	4.23×10^{-1}	3.00
256^2	1.99×10^{-5}	1.87	5.24×10^{-2}	3.01
512^2	8.45×10^{-6}	1.23	3.37×10^{-1}	−2.69
1024^2	1.41×10^{-6}	2.59	4.24×10^{-2}	2.99

Table 22 Example 3.3 perturbed tilted square. Maximum error for the solution and its gradients in the case where the ghost value is defined by a *linear* extrapolation and the interface location is found with a *quadratic* interpolant

Effective resolution	$\|u-u_h\|_\infty$	Order	$\|\nabla u-\nabla u_h\|_\infty$	Order
32^2	3.36×10^{-3}	–	1.18×10^{-1}	–
64^2	8.37×10^{-4}	2.01	9.31×10^{-2}	0.34
128^2	2.09×10^{-4}	2.00	3.76×10^{-2}	1.31
256^2	4.98×10^{-5}	2.07	1.85×10^{-2}	1.02
512^2	1.26×10^{-5}	1.98	1.01×10^{-2}	0.88
1024^2	3.22×10^{-6}	1.97	5.02×10^{-3}	1.00

Table 23 Example 3.3 perturbed tilted square. Maximum error for the solution and its gradients in the case where the ghost value is defined by a *quadratic* extrapolation and the interface location is found with a *linear* interpolant

Effective resolution	$\|u-u_h\|_\infty$	Order	$\|\nabla u-\nabla u_h\|_\infty$	Order
32^2	1.02×10^{-3}	–	6.10×10^{-2}	–
64^2	2.55×10^{-4}	2.00	3.36×10^{0}	−5.78
128^2	6.04×10^{-5}	2.08	4.19×10^{-1}	3.00
256^2	1.47×10^{-5}	2.04	5.23×10^{-2}	3.00
512^2	3.64×10^{-6}	2.01	3.37×10^{-1}	−2.69
1024^2	9.03×10^{-7}	2.01	4.25×10^{-2}	2.99

Table 24 Example 3.3 perturbed tilted square. Maximum error for the solution and its gradients in the case where the ghost value is defined by a *quadratic* extrapolation and the interface location is found with a *quadratic* interpolant

Effective resolution	$\|u-u_h\|_\infty$	Order	$\|\nabla u-\nabla u_h\|_\infty$	Order
32^2	8.90×10^{-4}	–	1.03×10^{-2}	–
64^2	2.26×10^{-4}	1.98	2.60×10^{-3}	1.99
128^2	5.71×10^{-5}	1.99	6.70×10^{-4}	1.96
256^2	1.43×10^{-5}	1.99	1.69×10^{-4}	1.99
512^2	3.59×10^{-6}	2.00	4.36×10^{-5}	1.96
1024^2	8.96×10^{-7}	2.00	1.07×10^{-5}	2.03

The L^∞ errors in the solution and gradient are presented in Tables 25 through 32. The highest resolution presented is 256^3 due to memory limitations for the simulation.

4 Synthesis of the Results

In this section, we analyze the order of accuracy and the error distribution of the solution gradients produced by the combination of (1) defining the ghost values with a linear or a quadratic extrapolation and (2) by finding the interface location with a linear or a quadratic interpolant. We also analyze the error distribution and the condition number of the asso-

Table 25 Example 3.4 centered sphere. Maximum error for the solution and its gradients in the case where the ghost value is defined by a *linear* extrapolation and the interface location is found with a *linear* interpolant

Effective resolution	$\|u-u_h\|_\infty$	Order	$\|\nabla u-\nabla u_h\|_\infty$	Order
32^3	7.98×10^{-3}	–	2.01×10^{-1}	–
64^3	1.98×10^{-3}	2.01	1.51×10^{-1}	0.41
128^3	5.05×10^{-4}	1.97	9.36×10^{-2}	0.69
256^3	1.26×10^{-4}	2.01	5.28×10^{-2}	0.83

Table 26 Example 3.4 centered sphere. Maximum error for the solution and its gradients in the case where the ghost value is defined by a *linear* extrapolation and the interface location is found with a *quadratic* interpolant

Effective resolution	$\|u-u_h\|_\infty$	Order	$\|\nabla u-\nabla u_h\|_\infty$	Order
32^3	1.07×10^{-2}	–	2.52×10^{-2}	–
64^3	2.66×10^{-3}	2.01	3.11×10^{-2}	−0.30
128^3	6.66×10^{-4}	2.00	2.44×10^{-2}	0.35
256^3	1.67×10^{-4}	2.00	1.59×10^{-2}	0.62

Table 27 Example 3.4 centered sphere. Maximum error for the solution and its gradients in the case where the ghost value is defined by a *quadratic* extrapolation and the interface location is found with a *linear* interpolant

Effective resolution	$\|u-u_h\|_\infty$	Order	$\|\nabla u-\nabla u_h\|_\infty$	Order
32^3	8.02×10^{-3}	–	2.37×10^{-1}	–
64^3	2.05×10^{-3}	1.97	1.63×10^{-1}	0.54
128^3	5.30×10^{-4}	1.95	1.04×10^{-1}	0.64
256^3	1.32×10^{-4}	2.00	5.99×10^{-2}	0.80

Table 28 Example 3.4 centered sphere. Maximum error for the solution and its gradients in the case where the ghost value is defined by a *quadratic* extrapolation and the interface location is found with a *quadratic* interpolant

Effective resolution	$\|u-u_h\|_\infty$	Order	$\|\nabla u-\nabla u_h\|_\infty$	Order
32^3	1.08×10^{-2}	–	2.23×10^{-2}	–
64^3	2.74×10^{-3}	1.97	5.67×10^{-3}	1.98
128^3	6.92×10^{-4}	1.99	1.56×10^{-3}	1.86
256^3	1.74×10^{-4}	1.99	4.10×10^{-4}	1.93

Table 29 Example 3.4 perturbed sphere. Maximum error for the solution and its gradients in the case where the ghost value is defined by a *linear* extrapolation and the interface location is found with a *linear* interpolant

Effective resolution	$\|u-u_h\|_\infty$	Order	$\|\nabla u-\nabla u_h\|_\infty$	Order
32^3	7.89×10^{-3}	–	2.98×10^{-1}	–
64^3	2.00×10^{-3}	1.98	2.02×10^{-1}	0.56
128^3	5.02×10^{-4}	2.00	1.07×10^{-1}	0.92
256^3	1.26×10^{-4}	2.00	5.51×10^{-2}	0.96

Table 30 Example 3.4 perturbed sphere. Maximum error for the solution and its gradients in the case where the ghost value is defined by a *linear* extrapolation and the interface location is found with a *quadratic* interpolant

Effective resolution	$\|u-u_h\|_\infty$	Order	$\|\nabla u-\nabla u_h\|_\infty$	Order
32^3	1.06×10^{-2}	–	9.39×10^{-2}	–
64^3	2.66×10^{-3}	1.99	1.62×10^{-1}	−0.79
128^3	6.66×10^{-4}	2.00	6.19×10^{-2}	1.39
256^3	1.66×10^{-4}	2.00	2.45×10^{-2}	1.34

Table 31 Example 3.4 perturbed sphere. Maximum error for the solution and its gradients in the case where the ghost value is defined by a *quadratic* extrapolation and the interface location is found with a *linear* interpolant

Effective resolution	$\|u-u_h\|_\infty$	Order	$\|\nabla u-\nabla u_h\|_\infty$	Order
32^3	7.97×10^{-3}	–	4.03×10^{-1}	–
64^3	2.08×10^{-3}	1.94	1.81×10^{0}	−2.17
128^3	5.26×10^{-4}	1.98	4.53×10^{-1}	2.00
256^3	1.33×10^{-4}	1.99	3.36×10^{-1}	0.43

Table 32 Example 3.4 perturbed sphere. Maximum error for the solution and its gradients in the case where the ghost value is defined by a *quadratic* extrapolation and the interface location is found with a *quadratic* interpolant

Effective resolution	$\|u-u_h\|_\infty$	Order	$\|\nabla u-\nabla u_h\|_\infty$	Order
32^3	1.07×10^{-2}	–	2.46×10^{-2}	–
64^3	2.74×10^{-3}	1.96	6.70×10^{-3}	1.88
128^3	6.92×10^{-4}	1.99	1.70×10^{-3}	1.98
256^3	1.74×10^{-4}	1.99	4.27×10^{-4}	1.99

ciated linear systems. In all cases, the solution is second-order accurate as demonstrated in [1, 6, 8]. We note that second-order accuracy is the maximum one can reach with the central difference scheme used.

4.1 Accuracy of Gradients

First, we look at the combination of a linear extrapolation for defining the ghost value and a linear interpolation to find the location of the interface. In this case we find that the gradients converge slowly (i.e. at most first order accurate) and their convergence rate oscillate as illustrated in Tables 1, 5, 9, 13, 17, 21, 25, and 29. We reach the same conclusion in the case where we use a quadratic interpolation to find the interface location, while still using a linear extrapolation in the definition of the ghost cell value as detailed in Tables 2, 6, 10, 14, 18, 22, 26, and 30.

Second, we consider defining the ghost value with a quadratic extrapolation. In this case the gradients are second-order accurate only if the location of the interface is found with an interpolant that is at least quadratic as demonstrated in Tables 4, 8, 12, 16, 20, 24, 28, and 32. The accuracy drops to first order at best (in average—also the convergence rates are oscillatory) in the case where the interface location is found with only a linear interpolant as shown in Tables 3, 7, 11, 15, 19, 23, 27, and 31.

We conclude that second-order accurate gradients can only be found by defining the ghost cell values with at least a quadratic extrapolation and finding the interface location with at least a quadratic interpolant.

4.2 Distribution of Error for the Solution and its Gradients

In general, the error of the gradient is largest close to the interface regardless of the order of interpolation for the interface location and extrapolation for the ghost values as illustrated in Fig. 5. Linear extrapolation for the ghost value produces larger errors in the solution close to the interface, while the error in the solution is smooth across all regions for quadratic extrapolation of the ghost value as depicted in Fig. 6. Defining the ghost values with a linear extrapolation, the gradient converge slowly (at most first-order accurate in average) even if we disregard the large errors contributed by the points within a small band near the interface as demonstrated for the case of the perturbed circle from Example 3.1 in Tables 33 through 36. This is characteristic of an Elliptic operator, for which errors propagate with infinite speed, and further supports our conclusion that a quadratic extrapolation for the ghost value is required for obtaining second-order accurate gradients.

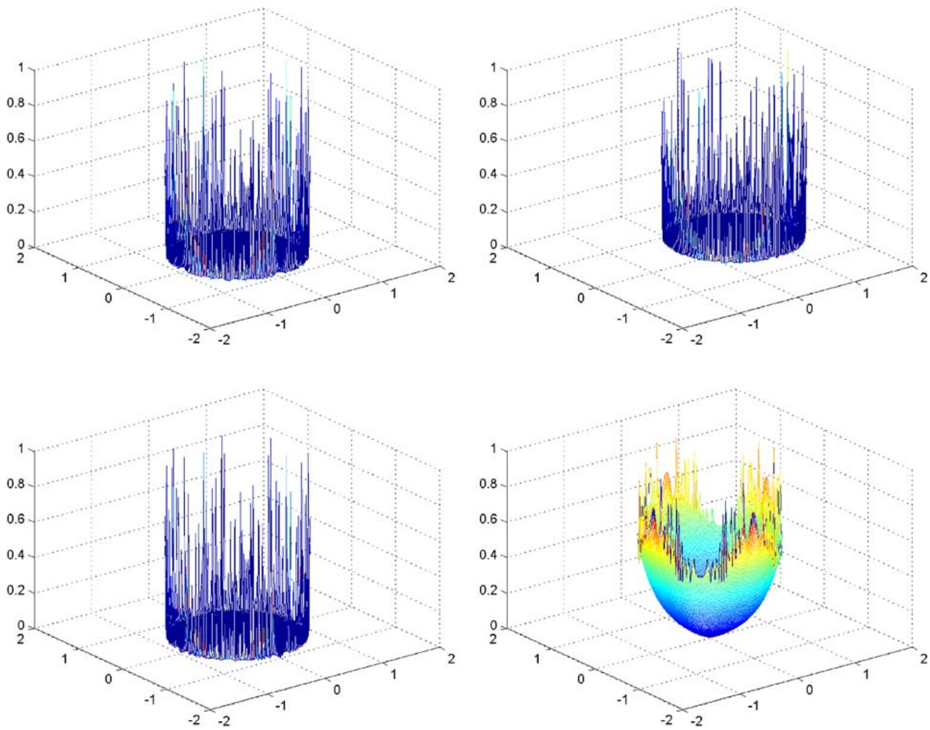

Fig. 5 Example 3.1 centered circle at 256^2 resolution. Normalized error for the gradients of the solution ∇u in the L^∞ norm. The ghost cell values are defined by linear extrapolation of the solution in *the top* figures and by quadratic extrapolation of the solution in *the bottom* figures. The interface location is found by linear interpolation ϕ in *the left* figures and by quadratic interpolation of ϕ in *the right* figures

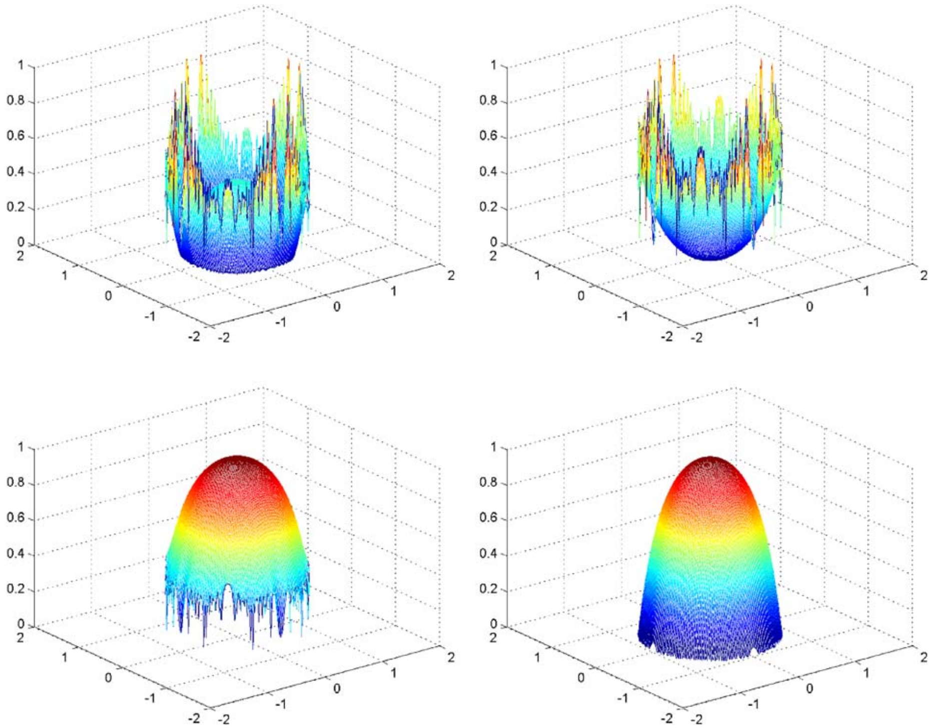

Fig. 6 Example 3.1 centered circle at 256^2 resolution. Normalized error for the solution u in the L^∞ norm. The ghost cell values are defined by linear extrapolation of the solution in *the top* figures and by quadratic extrapolation of the solution in *the bottom* figures. The interface location is found by linear interpolation of ϕ in *the left* figures and by quadratic interpolation of ϕ in *the right* figures

Table 33 Example 3.1 perturbed circle. Maximum error for the solution and its gradients in the case where the ghost value is defined by a *linear* extrapolation and the interface location is found with a *linear* interpolant, when points within a band of 0, 5, and 10 grid cell-width excluded near interface

Band	Effective resolution	$\|u-u_h\|_\infty$	Order	$\|\nabla u-\nabla u_h\|_\infty$	Order
0	256^2	1.11×10^{-4}	–	3.18×10^{-2}	–
	512^2	2.96×10^{-5}	1.91	1.66×10^{-2}	0.94
	1024^2	7.44×10^{-6}	1.99	8.35×10^{-3}	0.99
	2048^2	1.85×10^{-6}	2.00	4.19×10^{-3}	0.99
5	256^2	1.05×10^{-4}	–	4.70×10^{-4}	–
	512^2	2.68×10^{-5}	1.97	2.29×10^{-4}	1.04
	1024^2	6.91×10^{-6}	1.96	1.27×10^{-4}	0.85
	2048^2	1.69×10^{-6}	2.03	6.63×10^{-5}	0.94
10	256^2	1.05×10^{-4}	–	3.77×10^{-4}	–
	512^2	2.60×10^{-5}	2.01	1.08×10^{-4}	1.80
	1024^2	6.53×10^{-6}	1.99	5.75×10^{-5}	0.91
	2048^2	1.65×10^{-6}	1.98	3.07×10^{-5}	0.90

Table 34 Example 3.1 perturbed circle.. Maximum error for the solution and its gradients in the case where the ghost value is defined by a *linear* extrapolation and the interface location is found with a *quadratic* interpolant, when points within a band of 0, 5, and 10 grid cell-width excluded near interface

Band	Effective resolution	$\|u - u_h\|_\infty$	Order	$\|\nabla u - \nabla u_h\|_\infty$	Order
0	256^2	1.46×10^{-4}	–	1.33×10^{-2}	–
	512^2	3.62×10^{-5}	2.01	6.67×10^{-3}	1.00
	1024^2	9.10×10^{-6}	1.99	3.60×10^{-3}	0.89
	2048^2	2.28×10^{-6}	2.00	1.87×10^{-3}	0.94
5	256^2	1.46×10^{-4}	–	2.95×10^{-4}	–
	512^2	3.62×10^{-5}	2.01	1.09×10^{-4}	1.44
	1024^2	9.10×10^{-6}	1.99	6.25×10^{-5}	0.80
	2048^2	2.28×10^{-6}	2.00	3.32×10^{-5}	0.91
10	256^2	1.46×10^{-4}	–	2.93×10^{-4}	–
	512^2	3.62×10^{-5}	2.01	7.38×10^{-5}	1.99
	1024^2	9.10×10^{-6}	1.99	2.88×10^{-5}	1.36
	2048^2	2.28×10^{-6}	2.00	1.50×10^{-5}	0.94

Table 35 Example 3.1 perturbed circle. Maximum error for the solution and its gradients in the case where the ghost value is defined by a *quadratic* extrapolation and the interface location is found with a *linear* interpolant, when points within a band of 0, 5, and 10 grid cell-width excluded near interface

Band	Effective resolution	$\|u - u_h\|_\infty$	Order	$\|\nabla u - \nabla u_h\|_\infty$	Order
0	256^2	1.24×10^{-4}	–	2.77×10^{-2}	–
	512^2	3.10×10^{-5}	2.00	1.55×10^{-2}	0.84
	1024^2	7.77×10^{-6}	2.00	7.74×10^{-3}	1.00
	2048^2	1.96×10^{-6}	1.99	3.84×10^{-3}	1.01
5	256^2	1.24×10^{-4}	–	4.04×10^{-4}	–
	512^2	3.10×10^{-5}	2.00	1.58×10^{-4}	1.35
	1024^2	7.77×10^{-6}	2.00	7.29×10^{-5}	1.12
	2048^2	1.96×10^{-6}	1.99	3.55×10^{-5}	1.04
10	256^2	1.24×10^{-4}	–	3.18×10^{-4}	–
	512^2	3.10×10^{-5}	2.00	9.12×10^{-5}	1.80
	1024^2	7.77×10^{-6}	2.00	3.51×10^{-5}	1.38
	2048^2	1.96×10^{-6}	1.99	1.89×10^{-5}	0.90

4.3 Condition Number and Symmetry of the Linear Systems

Defining the ghost cell value with a linear extrapolation has one advantage over the quadratic extrapolation case: The linear system is symmetric, which allows the use of fast (and straightforward to implement) linear solvers like the preconditioned conjugate gradient [9, 16]. Indeed, the ghost value u_{i+1}^G is given by

$$u_{i+1}^G = \frac{u_I + (\theta - 1)u_i}{\theta} \tag{6}$$

Table 36 Example 3.1 perturbed circle. Maximum error for the solution and its gradients in the case where the ghost value is defined by a *quadratic* extrapolation and the interface location is found with a *quadratic* interpolant, when points within a band of 0, 5, and 10 grid cell-width excluded near interface

Band	Effective resolution	$\|u - u_h\|_\infty$	Order	$\|\nabla u - \nabla u_h\|_\infty$	Order
0	256^2	1.65×10^{-4}	–	2.61×10^{-4}	–
	512^2	4.14×10^{-5}	2.00	6.53×10^{-5}	2.00
	1024^2	1.04×10^{-5}	2.00	1.66×10^{-5}	1.98
	2048^2	2.60×10^{-6}	1.99	4.43×10^{-6}	1.91
5	256^2	1.65×10^{-4}	–	2.61×10^{-4}	–
	512^2	4.14×10^{-5}	2.00	6.52×10^{-5}	2.00
	1024^2	1.04×10^{-5}	2.00	1.63×10^{-5}	2.00
	2048^2	2.60×10^{-6}	1.99	4.27×10^{-6}	1.93
10	256^2	1.65×10^{-4}	–	2.61×10^{-4}	–
	512^2	4.14×10^{-5}	2.00	6.52×10^{-5}	2.00
	1024^2	1.04×10^{-5}	2.00	1.63×10^{-5}	2.00
	2048^2	2.60×10^{-6}	1.99	4.27×10^{-6}	1.93

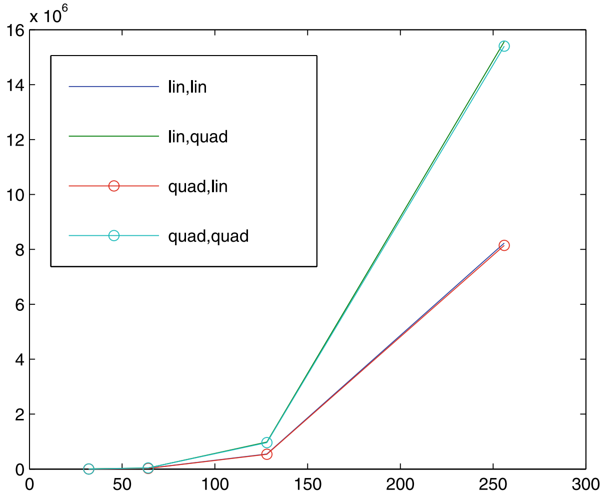

Fig. 7 Example 3.1 centered circle. Condition numbers versus the grid size. The four *curves* illustrate the impact of the extrapolation used to define the ghost values and the order of the interpolation for finding the interface location. The two (superimposed) *curves* with the smallest condition numbers are associated with the linear extrapolation for defining the ghost cells

and

$$u^G_{i+1} = \frac{2u_I + (2\theta^2 - 2)u_i + (-\theta^2 + \theta)u_{i-1}}{\theta^2 + \theta} \tag{7}$$

for linear and quadratic extrapolation respectively. Substituting u^G_{i+1} from (6) into (4) with $\beta = 1$ yields the symmetric discretization of

$$\frac{\frac{u_I}{\theta} - (1 + \frac{1}{\theta})u_i + u_{i-1}}{(\Delta x)^2} = f_i \tag{8}$$

while substituting (7) with $\beta = 1$ yields the non-symmetric discretization of

$$\frac{\frac{2u_I}{\theta^2+\theta} - \frac{2}{\theta}u_i + \frac{2}{\theta+1}u_{i-1}}{(\Delta x)^2} = f_i. \tag{9}$$

Also, observe that for linear extrapolation, the coefficient of u_i, which corresponds to the diagonal element of the matrix, is increased from 2 to $(1 + \frac{1}{\theta}) > 2$ since $\theta \in [0, 1]$. This increase in the diagonal element is beneficial for iterative methods to converge faster. In the case of a quadratic extrapolation, the diagonal element is increased by a factor of $\frac{1}{\theta}$ but the off-diagonal elements are also increased from 1 to $\frac{2}{\theta+1}$. In both cases the linear systems are diagonally dominant. Defining the ghost values with quadratic extrapolations produces consistently larger condition numbers in the matrices than in the case of a linear extrapolation, as demonstrated in Fig. 7 for the case of the centered circle from Example 3.1. Not surprisingly, the order of interpolation for finding the interface location has a negligible effect on the condition number.

5 Conclusions

We have presented numerical evidence for the order of accuracy that can be achieved by the Ghost-Fluid Method for Poisson equations on irregular domains with Dirichlet boundary conditions introduced by Gibou *et al.* [6, 8]. This paper can therefore serve as a guide on how to define ghost values and on how to define the interface location for those interested in the solution of Poisson problems on irregular domains. The same guide can be used for diffusion problems as well as Stefan-type problems. We have shown that a quadratic extrapolation for defining the ghost values and a quadratic interpolation for finding the interface location are necessary to obtain second-order accurate gradients, which in turn may be of interest when considering diffusion dominated moving boundary problems where the interface velocity is defined by the solution gradients. When linear approximation is used for either or both the extrapolation and the interpolation, the gradients converge slowly (at most first-order accurate in average and the convergence rate is oscillatory) across the entire domain, including at locations far away from the interface. In both cases the solution is second-order accurate. We also demonstrated that the symmetric discretization matrix produced by a linear extrapolation for the ghost value is significantly better conditioned relative to the non-symmetric discretization matrix produced by a quadratic extrapolation.

Acknowledgements The research of Y.-T. Ng, H. Chen and F. Gibou was supported in part by a Sloan Research Fellowship in Mathematics, by the National Science Foundation under grant agreement DMS 0713858 and by the Department of Energy under grant agreement DE-FG02-08ER15991. The research of C. Min was supported by the Korea Research Foundation Grant funded by the Korean Government (MOEHRD, Basic Research Promotion Fund) (KRF-2008-331-C00045).

References

1. Chen, S., Merriman, B., Osher, S., Smereka, P.: A simple level set method for solving Stefan problems. J. Comput. Phys. **135**, 8–29 (1997)

2. Chern, I.-L., Shu, Y.-C.: A coupling interface method for elliptic interface problems. J. Comput. Phys. **225**, 2138–2174 (2007)
3. Enright, D., Nguyen, D., Gibou, F., Fedkiw, R.: Using the particle level set method and a second order accurate pressure boundary condition for free surface flows. In: Proc. 4th ASME–JSME Joint Fluids Eng. Conf., number FEDSM2003-45144. ASME (2003)
4. Fedkiw, R., Aslam, T., Merriman, B., Osher, S.: A non-oscillatory Eulerian approach to interfaces in multimaterial flows (the ghost fluid method). J. Comput. Phys. **152**, 457–492 (1999)
5. Gibou, F., Chen, L., Nguyen, D., Banerjee, S.: A level set based sharp interface method for incompressible flows with phase change. J. Comput. Phys. **222**, 536–555 (2007)
6. Gibou, F., Fedkiw, R.: A fourth order accurate discretization for the Laplace and heat equations on arbitrary domains, with applications to the Stefan problem. J. Comput. Phys. **202**, 577–601 (2005)
7. Gibou, F., Fedkiw, R., Caflisch, R., Osher, S.: A level set approach for the numerical simulation of dendritic growth. J. Sci. Comput. **19**, 183–199 (2003)
8. Gibou, F., Fedkiw, R., Cheng, L.-T., Kang, M.: A second–order–accurate symmetric discretization of the Poisson equation on irregular domains. J. Comput. Phys. **176**, 205–227 (2002)
9. Golub, G., Loan, C.: Matrix Computations. The John Hopkins University Press, Baltimore (1989)
10. Jomaa, Z., Macaskill, C.: The embedded finite difference method for the Poisson equation in a domain with and irregular boundary and Dirichlet boundary conditions. J. Comput. Phys. **202**, 488–506 (2005)
11. Kang, M., Fedkiw, R., Liu, X.-D.: A boundary condition capturing method for multiphase incompressible flow. J. Sci. Comput. **15**, 323–360 (2000)
12. LeVeque, R., Li, Z.: The immersed interface method for elliptic equations with discontinuous coefficients and singular sources. SIAM J. Numer. Anal. **31**, 1019–1044 (1994)
13. Liu, X.D., Fedkiw, R., Kang, M.: A boundary condition capturing method for Poisson's equation on irregular domains. J. Comput. Phys. **154**, 151 (2000)
14. McCorquodale, P., Colella, P., Grote, D., Vay, J.-L.: A node-centered local refinement algorithm for Poisson's equation in complex geometries. J. Comput. Phys. **201**, 34–60 (2004)
15. Nguyen, D., Fedkiw, R., Kang, M.: A boundary condition capturing method for incompressible flame discontinuities. J. Comput. Phys. **172**, 71–98 (2001)
16. Saad, Y.: Iterative Methods for Sparse Linear Systems. PWS Publishing, New York (1996)